JOURNAL OF CATALYSIS 48, 386–394 (1977)

Kinetics of the Reduction of Uranium Oxide Catalysts

H. W. G. HEYNEN, C. G. M. M. CAMP-VAN BERKEL, AND H. S. VAN DER BAAN

Department of Chemical Technology, University of Technology, Eindhoven, The Netherlands

Received September 29, 1975; revised March 21, 1977

The reduction of uranium oxide and uranium oxide on alumina catalysts by ethylbenzene and by hydrogen has been studied in a thermobalance. Ethylbenzene mole fractions between 0.0026 and 0.052 and hydrogen mole fractions between 0.1 and 0.6 were applied at temperatures of 425–530°C. During the reduction the uranium oxides are converted into UO_2. The rate of reduction of pure uranium oxide appears to be constant in the composition region $UO_{2.6}$–$UO_{2.25}$. The extent of this region is independent of the concentration of the reducing agents and of the reaction temperature. The constant rate is explained in terms of a constant oxygen pressure which is in equilibrium with the two solid phases, U_3O_{8-x} and U_4O_9. The reduction rate is first order in hydrogen and zero order in ethylbenzene with activation energies of 120 and 190 kJ mol^{-1}, respectively. Oxygen diffusion through the lattice is probably not rate limiting. The reduction behavior of uranium oxide on alumina is different from that of pure uranium oxide; the rate of reduction continuously decreases with increasing degree of reduction. An explanation for this behavior has been given by visualizing this catalyst as a set of isolated uranium oxide crystallites with a relative wide variation of diameters, in an alumina matrix. At the beginning of the reduction, carbon dioxide and water are the only reaction products. Thereafter, benzene is found as well and, finally, at U/O ratios below 2.25, styrene also appears in the reactor outlet.

INTRODUCTION

Steenhof de Jong and co-authors (*1–3*) have described the dealkylation of toluene to benzene over bismuth uranate, Bi_2UO_6, at 400–500°C. Bismuth uranate acts as an oxidant and the toluene conversion stops when the uranate is reduced. Attempts to dealkylate ethylbenzene with the same compound were successful under similar reaction conditions, but the selectivity for benzene was less than 50%; other reaction products were CO_2, H_2O, H_2, styrene, and toluene. It turned out, however, that in this case the reaction does not stop when bismuth uranate is completely reduced to metallic bismuth and uranium dioxide but that styrene and hydrogen are then formed with high selectivity. Further investigation showed that for the latter reaction uranium dioxide is the active catalyst. The activity and the mechanical strength of the catalyst are greatly increased when uranium oxide is supported on alumina. The dehydrogenation of ethylbenzene and cumene over pure uranium dioxide and uranium dioxide on aluminum catalysts has been described elsewhere (*4–6*). In this paper we shall discuss the preparation of the active dehydrogenation catalysts, and attention will be focused on the reduction step. These reductions were carried out with ethylbenzene–nitrogen and with hydrogen–nitrogen mixtures in a thermobalance at 425–530°C.

EXPERIMENTAL

Preparation and Properties of the Catalysts

Pure uranium oxide (catalyst A). In order to obtain uranium oxide with a high surface

ISSN 0021-9517

TABLE 1

Properties of Catalysts A and B

Property	Pure uranium oxide Catalyst A	Uranium oxide on alumina Catalyst B
Color	Dark green	Orange-yellow
Oxygen/uranium ratio of the oxide	2.75	2.87
Uranium oxide content (wt%)	100	19.4
Specific surface area from BET using nitrogen adsorption ($m^2\ g^{-1}$)	6.3	144

TABLE 2

Thermobalance Reaction Conditions

Amount of oxide	70–80 mg
Particle size	0.15–0.30 mm
Mole fraction ethylbenzene	0.26–5.2 mol%
Nitrogen flow	13.3 liters h^{-1}
Reaction temperature	425–530°C
Pressure	Atmospheric

area, we used the following method of preparation. Uranyl acetate [$(CH_3COO)_2$-$UO_2 \cdot 2H_2O$, Merck p.a.] was dissolved in hot water. An excess of a concentrated ammonia solution was added and the yellow precipitate $UO_3 \cdot xNH_3 \cdot yH_2O$ was filtered off and washed with water. The precipitate was dried at 135°C for 24 hr and finally calcined at 600°C for 24 hr. The dark green product was broken up and sieved.

Uranium oxide on alumina (catalyst B). The precipitate $UO_3 \cdot xNH_3 \cdot yH_2O$, from 20 g of uranyl acetate, was prepared as described above. Aluminum nitrate [$Al(NO_3)_3 \cdot 9H_2O$, Merck p.a.], 409 g, was dissolved in water and poured into 300 ml of concentrated ammonia solution. The precipitate was filtered off and washed with water. The two precipitates were transferred to a flask, mixed with 1 liter of water and kept at 95–100°C with vigorous stirring. After 20 hr of stirring the solid was filtered off, washed with water, and dried for 24 hr at 135°C. Finally the product was calcined at 600°C in air for 24 hr, and the resulting catalyst was broken up and sieved.

Some properties of the catalysts are summarized in Table 1. The X-ray diffraction pattern of the pure uranium oxide showed α-U_3O_8 lines and very weak γ-UO_3 lines. Catalyst B was amorphous. The colors and the O/U ratios indicated that uranium oxide in catalysts A and B was mainly present as U_3O_8 and UO_3, respectively. We have not made X-ray diagrams of the solid phases formed during the reduction, because special techniques have to be applied, as rapid reoxidation of the

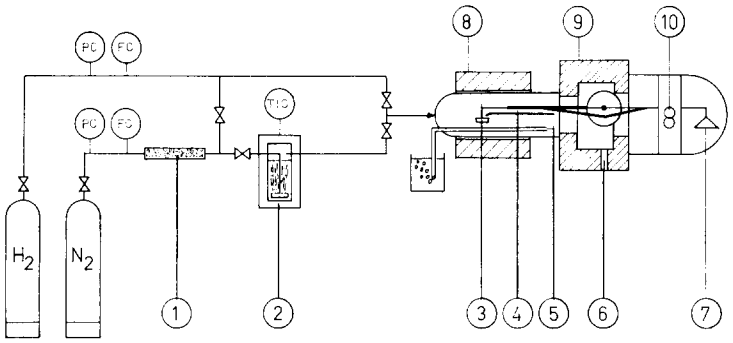

FIG. 1. Thermobalance: 1, BASF R3-11 catalyst; 2, vaporizer; 3, sample holder; 4, thermocouple; 5, gas outlet; 6, purge gas inlet; 7, counterweight pan; 8, furnace; 9, balance housing; 10, photovoltaic cells.

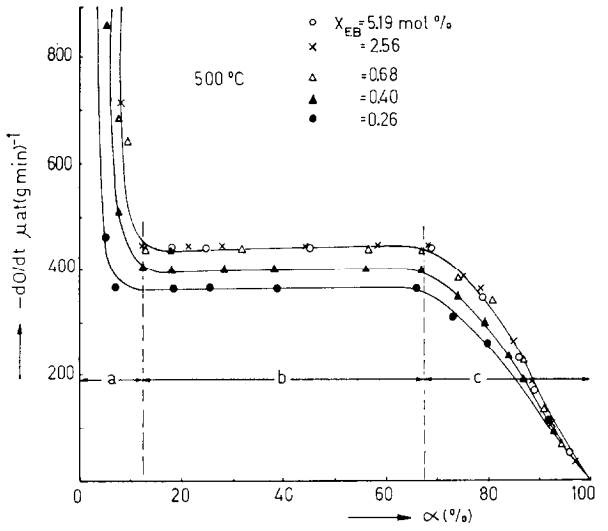

FIG. 2. Reduction rate as a function of the degree of reduction, α, at various ethylbenzene mole fractions.

material takes place even at room temperature.

From a pore size distribution determination of the alumina-supported catalyst using the Barrett, Joyner, and Halenda method with nitrogen as the adsorbate, we concluded that 90% of the pore volume consists of pores with a radius between 25 and 50 Å. From this experiment a surface area of 150 m^2 g^{-1} was found. This is in good agreement with the value given in Table 1, which was determined with an areameter.

Apparatus

Figure 1 shows the thermobalance and flow system. A constant flow of nitrogen, carefully freed of oxygen by reduced BASF R3-11 catalyst, is either passed through a thermostated vaporizer V, filled with ethylbenzene, or mixed with a constant flow of hydrogen. The desired ethylbenzene concentration in the reducing gas is established by adjusting the temperature of the vaporizer, which is controlled within 0.2°C. The mixture of nitrogen and reduction agent passes through the sample chamber of a DuPont Series 900/950 thermobalance. Experiments were carried out under isothermal conditions; the temperature is measured with a thermocouple just above the 5 × 10-mm platinum sample holder. To prevent back diffusion of air the exit tube of the apparatus ends under water.

The analytical system used to determine the gaseous reaction products has been described previously (*4*).

RESULTS AND DISCUSSION

Reduction of Pure Uranium Oxide (Catalyst A)

The conditions for the thermobalance experiments are given in Table 2. For both catalysts A and B no gas phase or pore diffusion limitations occur under these conditions, as the reduction rates are not affected by an increased gas flow or by an increase in the particle size. Neither does hydrocarbon adsorption influence the measurements since the maximum loss in weight attainable is the same for reduction with ethylbenzene and with hydrogen.

The degree of reduction (α) of the oxide is calculated from the recorded weight loss

of the solid as follows:

$$\alpha = \frac{\text{amount of oxygen removed from the uranium oxide}}{\text{largest amount of oxygen that can be withdrawn}}.$$

During reduction, catalyst A turns from green to black. Reduction with hydrogen gives the same color change. As on re-oxidation the original color returns, we conclude that the different colors must be ascribed to different stages of reduction.

The effect of the ethylbenzene concentration on the reduction of pure uranium oxide is shown in Fig. 2. In this figure three regions can be distinguished. In the first region (*a*) a very high, but rapidly declining, reduction rate occurs. This region ends at a catalyst composition $UO_{2.66}$ ($\alpha = 13\%$). In the next region (*b*) the reduction rate is constant for all ethylbenzene concentrations. This region ends at a catalyst composition $UO_{2.25}$ ($\alpha = 67\%$). Finally the rate decreases again in region *c*. The rate of reduction appears to be independent of the ethylbenzene mole fraction x_{EB} as long as this fraction is above 0.6 mol%. At the lowest mole fraction, 0.26 mol%, we calculate a reaction order of 0.2 in ethylbenzene.

The effect of the reaction temperature was studied at an ethylbenzene mole fraction of 0.68%. In Fig. 3 the rate of reduction as a function of the degree of reduction is given at various temperatures. Here again the three regions can be distinguished clearly, and we notice that the extent of region *b* ($13\% < \alpha < 67\%$) is also independent of the temperature. From the reduction rates in this region an activa-

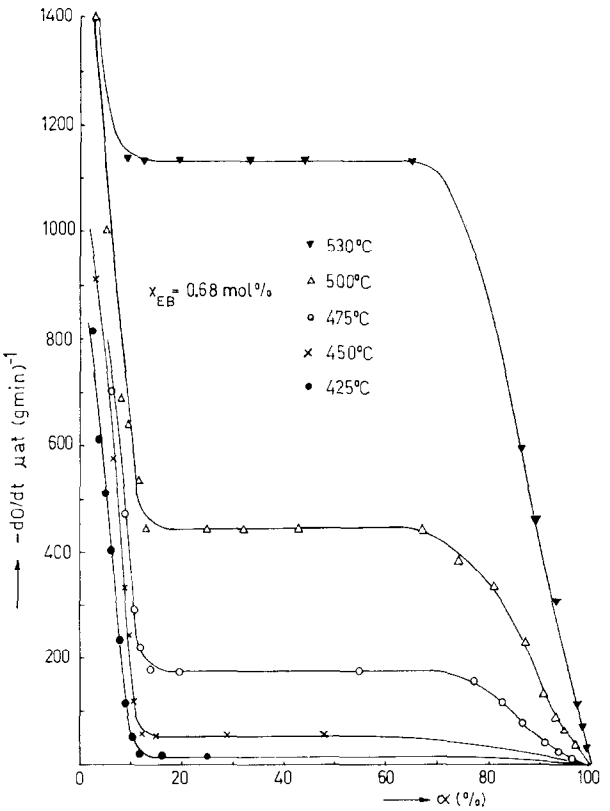

FIG. 3. Reduction rate as a function of the degree of reduction, α, at various temperatures: reduction with ethylbenzene.

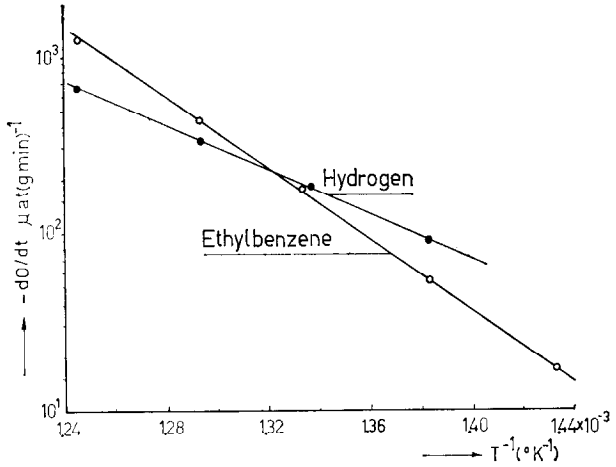

FIG. 4. Arrhenius plot: reduction rates in region *b* versus $1/T$. Ethylbenzene concentration, 0.68 mol%; hydrogen concentration, 30 mol%.

tion energy of 190 kJ mol^{-1} was calculated from Fig. 4.

For the reduction with hydrogen, mixtures of nitrogen and hydrogen containing 10 to 60 mol% of hydrogen were used. The other conditions were the same as those shown in Table 2. The results of the reduction of catalyst A with hydrogen are similar to those mentioned above. Again the reduction rate remains constant for $13\% < \alpha < 67\%$, but the reaction order for hydrogen is now very close to 1. The energy of activation (Fig. 4) is 120 kJ mol^{-1}.

A reduction behavior very similar to the above was noticed by Steenhof de Jong *et al.* (*1*, *2*) for the reduction of Bi_2UO_6 at low toluene concentrations. The appearance of different regions during the reduction of uranium trioxide is also mentioned by Notz and Mendel (*7*) and by Vlasov and Semavin (*8*, *9*).

For reduction with hydrogen Notz and Mendel (*7*) also found three regions with the same properties as we did, although the extent of the regions differs somewhat from ours. They found region *a* between $UO_{2.7}$ and $UO_{2.6}$ and region *b* between $UO_{2.6}$ and $UO_{2.2-2.1}$. According to Notz and Mendel (*7*) in region *a* a homogeneous transition from the upper to the lower composition limits of the orthorhombic α-U_3O_8 structure occurs [around 500°C these composition limits are $UO_{2.76}$ (U_3O_{8+x}) and $UO_{2.61}$ (U_3O_{8-x})]. In region *b*, U_3O_{8-x} is converted into the cubic α-U_4O_9 structure. Notz and Mendel (*7*) explain the constant rate by assuming chemisorption of hydrogen as a rate-limiting step, while oxygen diffuses through the solid to the surface as rapidly as it is abstracted. The final decrease in the rate is attributed to nonuniform crystallite size or poor gas accessibility to the centers of some large particles.

Vlasov and Semavin (*8*, *9*) also found a constant rate during the reduction of UO_3 by methane in the composition range $UO_{2.6} \rightarrow UO_{2.25}$; in this region the presence of two phases, namely, an orthorhombic U_3O_{8-x} phase and a cubic U_4O_9 phase, is noted. The existence of a composition range in which the rate depends little on the degree of reduction is ascribed by these authors to "the similarity of certain physical properties of the U_3O_{8-x} and U_4O_9 phases." However, we believe that the constant reduction rate in region *b* can be explained by simple application of the phase rule. Because in region *b* two solid phases with clearly different crystal

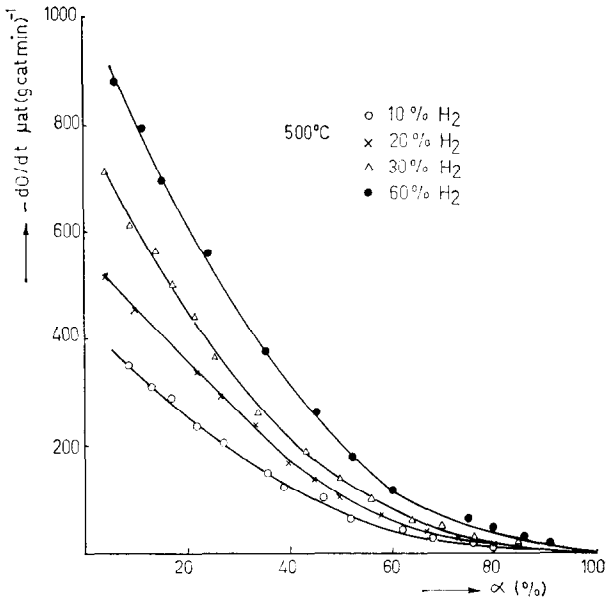

FIG. 5. Reduction rate as a function of the degree of reduction, α, at various hydrogen mole fractions; catalyst B.

structures are present, at a fixed temperature no degree of freedom is left. This results in a constant oxygen activity in the thermodynamic sense; i.e., there is a constant oxygen pressure in equilibrium with the system. At the beginning of

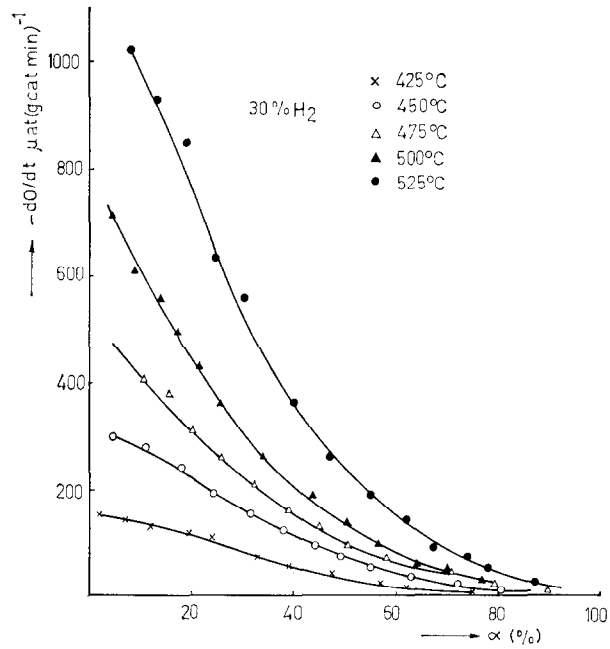

FIG. 6. Reduction rate as a function of the degree of reduction, α, at various temperatures: catalyst B, reduction with hydrogen.

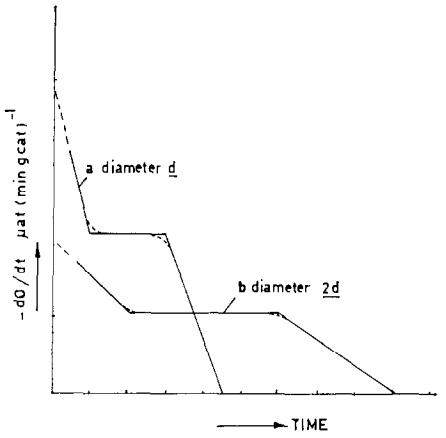

FIG. 7. Relation between reduction rate and crystallite size.

region *c* a constant rate would also be expected, because U_4O_9 and UO_{2+x} are present. However, this is not found. One explanation for this is that this reduction is a kinetically limited process in which a layer of UO_{2+x} is formed around a core of unreacted U_4O_9. Another possible explanation is that, because the U_4O_9 lattice is an oxygen excess superlattice of UO_{2+x}, as far as the oxygen activity is concerned, U_4O_9 and UO_{2+x} can be considered as one phase.

The different activation energies and reaction orders and rates that we found for the reductions with hydrogen and ethylbenzene can only be explained when the oxygen diffusion is not the rate-determining step. This conclusion is also supported by the work of Vlasov and Semavin (*8*, *9*) and by data on the mobility of oxygen in uranium oxide lattices, determined by isotopic exchange (*10*). The zero order for ethylbenzene indicates that the active catalyst surface is almost completely occupied and probably that the chemical reaction is rate determining. The first order for hydrogen indicates that the chemisorption is rate determining in this case. That the kinetics of the hydrogen reduction of UO_3 were best interpreted in terms of hydrogen chemisorption as a rate-controlling step was also observed by De Marco and Mendel (*11*), Morrow *et al.* (*12*) and Dell and Wheeler (*13*).

Reduction of Uranium Oxide on Alumina (Catalyst B)

These experiments were carried out under the same conditions as mentioned above. However, only hydrogen reductions could be carried out accurately. When ethylbenzene is led over this large surface area catalyst, the rate in the beginning of the reduction cannot be determined accurately as the hydrocarbon adsorption rate and the oxygen depletion rate are comparable initially.

The results of the reduction of catalyst B with hydrogen are shown in Figs. 5 and 6. The reduction behavior of this catalyst is different from that of catalyst A. None of the usually applied kinetic expressions for gas solid reactions fits these experimental data, situations such as, for instance, the "shrinking core" relation (*14*), the product

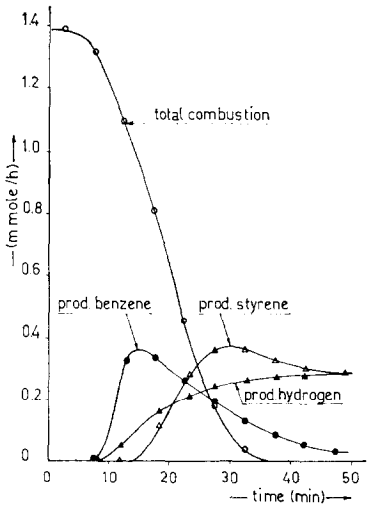

FIG. 8. Product composition change during the reduction of catalyst A in a tubular reactor: reaction temperature, 490°C; catalyst weight, 3.90 g; feed, 1.39 mmol hr^{-1} ethylbenzene and 144 mmol hr^{-1} nitrogen.

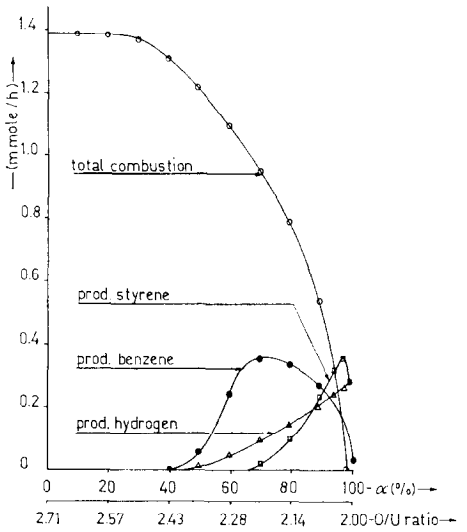

FIG. 9. Product composition change as a function of the average degree of reduction and of the overall O/U ratio of catalyst A: conditions as in Fig. 8.

layer diffusion models applicable to reactions of the type A(gas) + B(solid) → P(gas) + Q(solid) (*15*, *16*), or the models in which, besides the reaction, oxygen diffused through the lattice is also incorporated (*2*, *17*).

We suppose that catalyst B consists of crystallites of uranium oxide on alumina or in an alumina matrix and that no solid-state reaction takes place between uranium oxide and alumina. The most important reason for this assumption is that the catalytic properties of uranium oxide, regarding the ethylbenzene dehydrogenation, do not change when the uranium oxide is brought in contact with alumina.

Comparison of the hydrogen reduction curves of both catalyst A and catalyst B shows that the average reduction rates, expressed in microatoms of O · (minutes · grams of catalyst)$^{-1}$, are in the same range. Therefore, in spite of the fact that the BET surface area is about 150 m^2 g^{-1}, the active reduction surface area of catalyst B is about the same as of pure uranium oxide, namely, 6 m^2 g^{-1}. Reduction of samples of catalyst A having different surface areas showed that the rate of reduction, expressed as noted above, is proportional to the surface area or inversely proportional to the average crystallite diameter. This is represented schematically in Fig. 7. From this figure we see that the average reduction rate of a catalyst, with a particle diameter distribution relatively wide in comparison to its average diameter, turns into a continuously decreasing curve, as was found for catalyst B. We feel that a description of catalyst B as a set of isolated uranium oxide crystallites in alumina is appropriate, as the alumina matrix will act as a barrier to the oxygen transport from one crystallite to the other, while in pure uranium oxide this transport can occur via planes of contact of the crystallites.

Reaction between Ethylbenzene and Uranium Oxide in a Tubular Flow Reactor

The composition of the gaseous reaction products formed during a typical reduction of catalyst A by ethylbenzene in a tubular flow reactor is shown in Fig. 8. The reaction starts with complete combustion of ethylbenzene to carbon dioxide and water. As in the first minutes the conversion to CO_2 and H_2O is 100%, it can be expected that the degree of reduction of the catalyst is higher in the upstream part of the reactor than in the more downstream part. After some time, the formation of benzene by oxidative dealkylation is observed, while styrene formation starts somewhat later. Hydrogen, formed together with the styrene, is partly oxidized to water but after completion of the reduction the amounts of hydrogen and styrene in the product are equal. The partial oxidation of hydrogen causes the maximum in the styrene production curve, as this oxidation shifts the dehydrogenation equilibrium toward styrene.

The amount of oxygen removed from the catalyst was calculated from the quantities

of the various products assuming the following reactions:

$$C_8H_{10} + 21[O] \rightarrow 8CO_2 + 5H_2O,$$

$$C_8H_{10} + 6[O] \rightarrow C_6H_6 + 2CO_2 + 2H_2O,$$

$$C_8H_{10} + [O] \rightarrow C_8H_8 + H_2O,$$

and thus the course of the overall O/U ratio of the catalyst as shown in Fig. 9 was determined. The total amount of oxygen removed from the catalyst was calculated to be 0.70 matom/mmol of uranium oxide. This is in good agreement with the amount of 0.71 matom/mmol calculated from the thermobalance experiments (see Table 1).

In Fig. 9 the productivities of the various reaction products are given as a function of the degree of reduction of catalyst A and as a function of the O/U ratio of the oxide. This figure shows that the feed is completely oxidized in region *a*. The amount of ethylbenzene which is oxidized to carbon dioxide and water gradually decreases in the regions *b* and *c*. The partial oxidation of ethylbenzene to benzene starts in the middle of region *b* and is a maximum at the transition from region *b* to region *c*. At this transition point the production of styrene starts and increases gradually in this last region, *c*.

During reduction of catalyst B the hydrocarbon product composition changes in a way similar to that described for catalyst A.

REFERENCES

1. Steenhof, de Jong, J. G., Guffens, C. H. E., and van der Baan H. S., *J. Catal.* **26**, 401 (1972).
2. Steenhof de Jong, J. G., Guffens, C. H. E., and van der Baan, H. S., *J. Catal.* **31**, 149 (1973).
3. De Jong, J. G., and Batist, P. A., *Rec. Trav. Chim. Pays-Bas* **90**, 749 (1971).
4. Heynen, H. W. G., and van der Baan, H. S., *J. Catal.* **34**, 167 (1974).
5. Heynen, H. W. G., and van der Baan, H. S., *Advan. Chem. Ser.* **133**, 67 (1974).
6. Heynen, H. W. G., Thesis. Eindhoven, 1974.
7. Notz, K. J., and Mendel, M. G., *J. Inorg. Nucl. Chem.* **14**, 55 (1960).
8. Vlasov, V. G., and Semavin, Yu. N., *J. Appl. Chem. USSR* **40**, 374 (1967).
9. Vlasov, V. G., and Semavin, Yu. N., *J. Appl. Chem. USSR* **40**, 1169 (1967).
10. Johnston, F. J., Hutchison, D. A., and Katz, J. J. *J. Inorg. Nucl. Chem.* **7**, 392 (1958).
11. De Marco, R. E., and Mendel, M. G., *J. Phys. Chem.* **64**, 132 (1960).
12. Morrow, S. A., Graves, S., and Tomlinson, L. *Trans. Faraday Soc.* **57**, 1400 (1961).
13. Dell, R. M., and Wheeler, V. J., *J. Phys. Chem.* **64**, 1590 (1960).
14. Levenspiel, O., "Chemical Reaction Engineering." Wiley, New York, 1962.
15. Massoth, F. E., and Scarpiello, D. A., *J. Catal.* **21**, 225 (1971).
16. Seth, B. B. L., and Ross, H. U., *Trans. Met. Soc. AIME* **233**, 180 (1965).
17. Batist, Ph. A., Kapteyns, C. J., Lippens, B. C., and Schuit, G. C. A., *J. Catal.* **7**, 33 (1967).